Ocean Dynamics (2010) 60:791–801
DOI 10.1007/s10236-010-0288-0

# Mechanisms of the meridional heat transport in the Southern Ocean

**Denis L. Volkov · Lee-Lueng Fu · Tong Lee**

Received: 18 December 2009 / Accepted: 11 April 2010 / Published online: 29 April 2010


**Abstract** The Southern Ocean (SO) transports heat towards Antarctica and plays an important role in determining the heat budget of the Antarctic climate system. A global ocean data synthesis product at eddy-permitting resolution from the Estimating the Circulation and Climate of the Ocean, Phase II (ECCO2) project is used to estimate the meridional heat transport (MHT) in the SO and to analyze its mechanisms. Despite the intense eddy activity, we demonstrate that most of the poleward MHT in the SO is due to the time-mean fields of the meridional velocity, $V$, and potential temperature, $\theta$. This is because the mean circulation in the SO is not strictly zonal. The Antarctic Circumpolar Current carries warm waters from the region south of the Agulhas Retroflection to the lower latitudes of the Drake Passage and the Malvinas Current carries cold waters northward along the Argentinian shelf. Correlations between the time-varying fields of $V$ and $\theta$ (defined as transient processes) significantly contribute to the horizontal-gyre heat transport, but not the overturning heat transport. In the highly energetic regions of the Agulhas Retroflection and the Brazil-Malvinas Confluence the contribution of the horizontal transient processes to the total MHT exceeds the contribution of the mean horizontal flow. We show that the southward total MHT is mainly maintained by the meridional excursion of the mean geostrophic horizontal shear flow (i.e., deviation from the zonal average) associated with the Antarctic Circumpolar Current that balances the equatorward MHT due to the Ekman transport and provides a net poleward MHT in the SO. The Indian sector of the SO serves as the main pathway for the poleward MHT.

**Keywords** Southern Ocean · Meridional heat transport · Antarctic circumpolar current · Eddy-induced heat transport · Meridional overturning circulation · Horizontal gyre transport · Eddy-induced heat transport

Responsible Editor: Dirk Olbers

D. L. Volkov (✉)
Joint Institute for Regional Earth System Science and Engineering, University of California Los Angeles, Los Angeles, CA, USA
e-mail: denis.volkov@jpl.nasa.gov

D. L. Volkov · L.-L. Fu · T. Lee
Jet Propulsion Laboratory, California Institute of Technology, Pasadena, CA, USA

## 1 Introduction

The Southern Ocean (SO) circulation plays an important role in the Earth's climate system by transporting heat from mid- to high latitudes of the Southern Hemisphere. It is dominated by the eastward flowing Antarctic Circumpolar Current (ACC), which is the largest current on Earth with an observed average mass transport across the Drake Passage of about 140 Sv (1 Sv=$10^6$m$^3$/s; e.g., Cunningham et al. 2003; Whitworth and Peterson 1985). The heat carried by the ACC waters affects the climate of Antarctica. Antarctica is the Earth's biggest reservoir of fresh water, contained in glaciers, and changes in its climate have prominent global consequences.

Strong westerly winds over the SO impart eastward momentum to the ocean and drive the equatorward Ekman transport near the surface. The Ekman transport creates an overturning cell that carries heat equatorward. It has been established that the wind stress over the SO is mostly balanced by the bottom form stress due to pressure differences across topography, as first suggested by Munk and Palmén (1951) and then confirmed by observations (Bryden and Heath 1985; Phillips and Rintoul 2000) and models (Ivchenko et al. 1996; Stevens and Ivchenko 1997; Olbers and Ivchenko

2001). In terms of the meridional overturning circulation (MOC), this means that the northward Ekman flux is balanced by a geostrophic southward flow, supported by zonal pressure differences (Rintoul et al. 2001). To maintain the heat balance of the SO there must be an associated poleward transfer of heat.

It is widely acknowledged that mesoscale eddies in the SO play an important role in transporting heat poleward (e.g., Bryden 1979; de Szoeke and Levine 1981; Thompson 1993; Phillips and Rintoul 2000; Jayne and Marotzke 2002; Meijers et al. 2007; Volkov et al. 2008a) and momentum downward across density surfaces (Johnson and Bryden 1989). In the absence of the mean meridional geostrophic flow across the Drake Passage, for example, eddies must carry the bulk of heat poleward to balance the heat loss to the atmosphere at higher latitudes in the region. The importance of eddy fluxes has been demonstrated by the residual-mean theory (Marshall and Radko 2003; Karsten et al. 2002; Karsten et al. 2002) in the context of coarse-resolution models. According to the theory, the Ekman-driven MOC is balanced by an eddy-induced overturning cell of an opposite sign and heat is carried poleward by the residual flow.

There has been much discussion on the use of the streamwise and zonal coordinates for studying the dynamics of the ACC (e.g., Ivchenko et al. 1996; Lee and Coward 2003). The former was found to be beneficial to understanding the momentum balance of the ACC (Ivchenko et al. 1996) and estimating *cross-stream* eddy heat fluxes. De Szoeke and Levine (1981) used a hydrographic climatology to calculate the mean advective geostrophic heat flux across a circumpolar path of constant vertically averaged temperature close to the Polar Front of the ACC. They showed that there is almost no net heat carried by mean geostrophic flows across this path and most of the heat is transported by eddies. Thompson (1993) repeated these calculations using the output of the Fine Resolution Antarctic Model (FRAM) and arrived at the same conclusion. However, when he estimated the heat transport across the section at 55.25° S he found the total heat transport of −0.15 PW (1 PW=$10^{15}$ W) was almost equally contributed by the mean flow (−0.08 PW) and by mesoscale transient processes (−0.07 PW). It is, therefore, important to distinguish the concept of heat transport across the path of the ACC from the concept of heat transport across a latitude circle. The latter is referred to as the *meridional* heat transport (henceforth the MHT).

While the *cross-stream* heat transport can better elucidate the effect of eddies in transporting heat across the stream, the MHT is a more suitable quantity for the study of the ocean and atmosphere heat transport as a whole. Sun and Watts (2002) argued that while it is correct to say that mean geostrophic motions carry little heat across the ACC, it is not appropriate to assess the contribution of the ACC in the MHT of the SO solely based on streamline paths. It is not surprising that there is little heat flux carried by the mean flow across such paths, because the time-mean globally meandering pattern of the ACC and its correlation with zonally varying ocean temperature is missing in the calculation. Analyzing a historical hydrographic climatology Sun and Watts (2002) found that the mean baroclinic geostrophic flow relative to 3,000 m carries a significant amount of heat poleward: −0.140±0.010 PW across 56° S, −0.095±0.009 PW across 58° S, and −0.082±0.008 PW across 60° S. In the residual-mean concept the contribution of the mean flow is either missing when fluxes are integrated along the ACC or it is included in the overturning circulation together with eddy fluxes in the case of a zonal integration.

Despite the past efforts, the heat transport of the SO remains a poorly observed quantity. Existing observational data are still too limited. Synoptic hydrographic surveys do not resolve the seasonal and higher frequency variability that may alias into the mean estimates. The contribution of transient processes arising from correlations between the time-varying fields of temperature and meridional velocity (mesoscale eddies and meandering of the ACC, variability of the ACC transport, the variability of the upper-ocean Ekman transport etc.) is, therefore, difficult to estimate. Simulations by ocean general circulation models (OGCMs) often lack observational constraints and many of them do not adequately represent mesoscale eddies.

In this paper we present estimates of the MHT of the SO using a high-resolution global-ocean and sea-ice data synthesis at eddy-permitting resolution from the Estimating the Circulation and Climate of the Ocean, Phase II (ECCO2) project (www.ecco2.org). We believe that the transfer of heat across latitude circles is key to understanding the meridional migration of the ACC and associated isotherms in the SO. In fact, in an idealized ocean without zonal boundaries there would be no heat carried meridionally by the mean flow, the time-mean isotherms would be zonal and all the MHT would be accomplished by eddies.

The main objective of this study is to discuss the mechanisms of the MHT in the SO, in particular, the relative contributions by the overturning and horizontal circulations. To complement previous studies, we will also separate the effect of the time-mean gyre (ACC) from the effect of the transients (combined effect of eddies and other variability). A unique feature of the study is the use of a high-resolution model constrained by available observations. As will be shown in the next section, the model results have realistically reproduced the mesoscale variability of the SO that is important to the MHT.

## 2 ECCO2 data synthesis

### 2.1 The model

The ECCO2 project aims to produce accurate, physically consistent, time-evolving syntheses of most available global-scale ocean and sea-ice data at eddy-permitting resolution. An ECCO2 data synthesis is obtained by least-squares fit of a global full-depth-ocean and sea-ice configuration of the Massachusetts Institute of Technology OGCM (Marshall et al. 1997) to the available satellite and in situ data. This least-squares fit is carried out for a small number of control parameters using a Green's function approach (Menemenlis et al. 2005). The control parameters include initial temperature and salinity conditions, atmospheric surface boundary conditions, background vertical diffusivity, critical Richardson numbers for the Large et al. (1994) KPP scheme, air–ocean, ice–ocean, air–ice drag coefficients, ice/ocean/snow albedo coefficients, bottom drag, and vertical viscosity. Data constraints include sea level anomaly, time-mean sea level, sea surface temperature, vertical temperature and salinity profiles, and sea-ice concentration, motion, and thickness. The solution requires the computation of a number of sensitivity experiments that are free, unconstrained calculations by a forward model. The experiments are designed to adjust the model parameters, forcing, and initial conditions. Then the model is run forward again using the adjusted parameters, free of any constraints, as in any ordinary model simulation. The period of the model run used in this study is 10 years (from January 1992 to January 2002). The model employs a cube-sphere grid projection. Each face of the cube comprises 510 by 510 grid cells with a mean horizontal grid spacing of 18 km. There are 50 vertical layers with thicknesses ranging from 10 m at the surface to 456 m near the bottom. This model configuration permits mesoscale eddies.

### 2.2 The Southern Ocean circulation

Displayed in Fig. 1a is a snapshot of the absolute velocity in the upper level at 5 m depth. It demonstrates a highly variable circulation in the SO complicated by meanders, filaments, and eddies. The model-simulated ACC appears to be a multiple jet system, which is consistent with observations (e.g., Rintoul et al. 2001) and other high-resolution models, for example, the FRAM (Webb et al. 1991; Ivchenko et al. 1996), the Parallel Ocean Program model (Olbers and Ivchenko 2001), the more recent Southern Ocean State Estimate (Mazloff et al. 2010) etc. The number of jets in the ACC system is maximum in the Atlantic and Indian sectors of the SO, gradually decreasing towards the relatively narrow gap of Drake Passage. As demonstrated by the barotropic streamfunction (Fig. 1b), the ECCO2-simulated average transport of the ACC across the Drake Passage is 142 Sv. This estimate compares well with observations (Cunningham et al. 2003; Whitworth and Peterson 1985). The eastward transport south of Tasmania increases to 158 Sv owing to the recirculation of the Indonesian throughflow water, which is consistent with 157±10 Sv estimate of Ganachaud and Wunsch (2000).

The mesoscale variability is rather well represented by the model. Figure 2 demonstrates the comparison of the altimetry[1]- and ECCO2-derived mean surface eddy kinetic energies (EKE). Only EKE greater than 100 $cm^2/s^2$ is shown. The model-simulated ACC path associated with elevated EKE agrees well with altimetry. Major energetic regions of the SO such as the Brazil-Malvinas Confluence in the South Atlantic, the Agulhas Retroflection and the ACC drift in the Indian sector of the SO, and the local EKE maximum south of Tasmania, are well reproduced. The ACC path is strongly influenced by topographic features (contours in Fig. 2). In most cases the ACC tends to avoid topographic obstacles with depth less than 3,000 m. All these indicate that the ECCO2 model adequately captures the interactions between the flow and the topographic features due to the topographic form stresses. The comparisons of the ECCO2 model with altimetry demonstrating eddy interactions with the mean flow and topography can be found in Fu (2009).

As demonstrated in Fig. 3, between 30° S and 60° S the model-derived zonally averaged EKE differs from the altimetry-derived zonally averaged EKE by a factor of 1.4 on average. This is a reasonable match compared to coarser resolution eddy-permitting models used to study heat transport. For example, Jayne and Marotzke (2002) reported that EKE in 1/4° resolution Parallel Ocean Climate Model (POCM) was too weak compared to altimetry by at least a factor of 4. The large peaks of zonally averaged altimetry- and ECCO2-derived EKE at 35–45° S (Fig. 3) correspond to the Agulhas Retroflection region and to the Brazil-Malvinas Confluence—some of the most energetic regions in the ocean. Peaks at 49° S in altimetry and ECCO2 zonally averaged EKE are associated with the ACC jet just south of the Zapiola Anticyclone (centered at 45° S and 45° W) in the Argentine Basin and with the ACC drift in the Indian sector of the SO crossing this latitude. Other major peaks at 59° W are related to elevated mesoscale activity south of Tasmania and New Zealand. It should be noted that the AVISO merged altimetry product still underestimates the real EKE of the ocean because of the

[1] Merged altimeter product produced by SSALTO/DUACS and distributed by AVISO with support from CNES (www.aviso.oceanobs.com) was used (SSALTO/DUACS user handbook 2009).

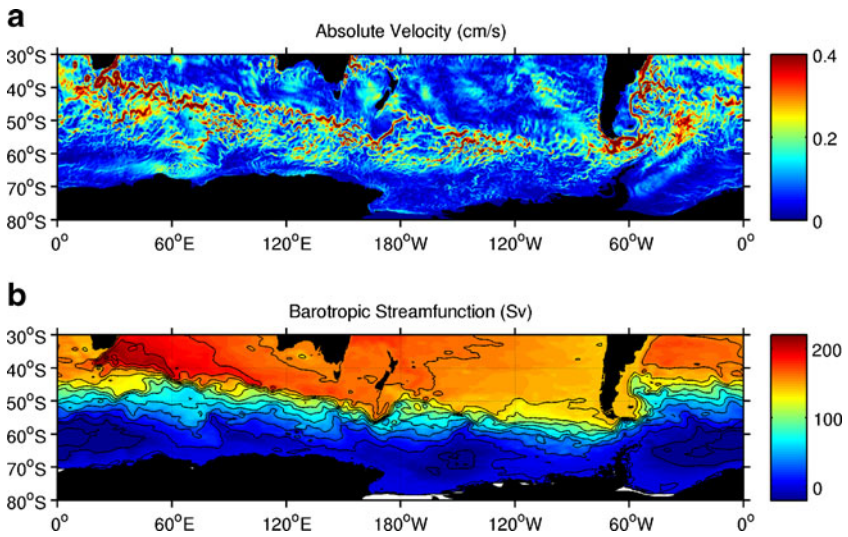


**Fig. 1** **a** A typical snapshot of the absolute velocity at 5 m depth (cm/s) and **b** the time-mean barotropic streamfunction (Sv)

limited sampling by existing altimeters. The presence of a strong eddy field, weak stratification, and small Rossby deformation radius, which ranges from ~30 km at 40° S to less than 10 km near Antarctica (Chelton et al. 1998), represent a formidable technical challenge to resolve eddy scales in the SO. Therefore, the ECCO2 model with its mean horizontal resolution of 18 km permits, but does not fully resolve eddies.

## 3 Methodology

The product of the meridional velocity $V=V(x,y,z,t)$ and potential temperature $\theta=\theta(x,y,z,t)$ integrated over depth and zonally in the absence of the net mass flux across a given latitude circle $y$ at time $t$ represents the MHT, denoted by $Q(y,t)$ (Hall and Bryden 1982; Bryan 1982):

$$Q(y,t) = \iint \rho C_p V\ \theta\ dz\ dx, \tag{1}$$

where $\rho$ is the potential density of seawater, and $C_p$ is the specific heat capacity of seawater at constant pressure. When the net mass flux is present, then $Q$ becomes dependent on the temperature scale (e.g., degree Celsius or Kelvin) and is called temperature flux (Montgomery 1974). The time-mean MHT can be decomposed as follows (Bryan 1982):

$$\overline{Q}(y) = \iint \rho C_p \left\{ [\overline{V}][\overline{\theta}] + \overline{[V'][\theta']} + (\overline{V})(\overline{\theta}) + \overline{(V')(\theta')} \right\} dz dx, \tag{2}$$

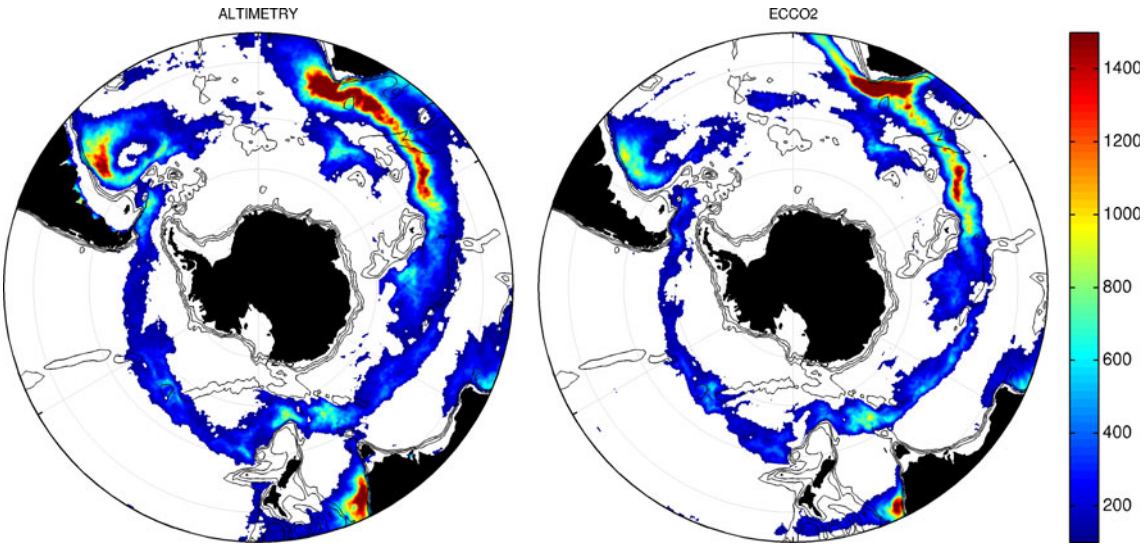


**Fig. 2** Ten-year mean surface eddy kinetic energy ($cm^2/s^2$) from satellite altimetry observations (*left*) and the ECCO2 output (*right*). Only values larger than 100 $cm^2/s^2$ are shown. Contours outline bottom topography from 1,000 to 3,000 m depth with the separation between the isobaths of 1,000 m

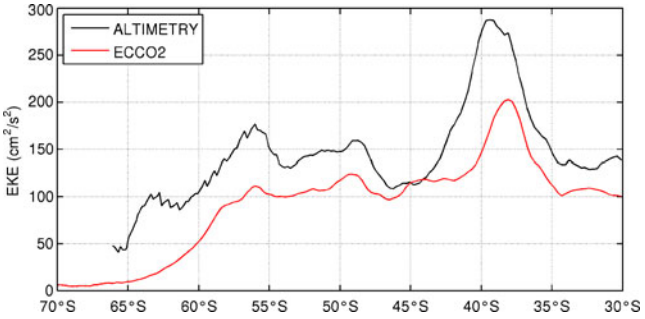


**Fig. 3** Zonally averaged eddy kinetic energy ($cm^2/s^2$) derived from satellite altimetry (*black curve*) and ECCO2 data synthesis (*red curve*)

where the overbar indicates averaging over the 10-year period of the study, $\overline{V}$, $\overline{\theta}$ are the time-mean meridional velocity and potential temperature, are $V'$, $\theta'$ the deviations from the time mean, [·] represents the zonal average, and (·) represents the deviation from the zonal average.

The components of the sum inside the integral in (2) are the MHT due to the time-mean overturning circulation, the MHT due to the transient processes in the overturning circulation, the MHT due to the time-mean horizontal circulation (oceanic gyres), and the MHT due to the transient processes in the horizontal circulation (eddies and seasonal/interannual variability of oceanic gyres). We use the term "transient processes" here to indicate contribution from correlations between the time-varying fields of $V$ and $\theta$ associated with both the overturning and the horizontal circulations.

Because of data storage constraints only monthly averages of $V$ and $\theta$, and monthly averages of the product $V\times\theta$, computed from initial 6-hourly $V$ and $\theta$, are saved by the model. Therefore, the decomposition in (2) has an error caused by missing the terms related to the intra-monthly variability of $V$ and $\theta$. This missing term will be discussed below. The transient processes included in (2) represent the correlation between the inter-monthly variability of $V$ and $\theta$.

## 4 Mechanisms

### 4.1 Meridional overturning circulation

It is instructive to discuss the MOC because it plays an important role in the MHT. Displayed in Fig. 4 is the Eulerian mean (zonally integrated) MOC streamfunction in depth coordinate from 70° S to 30° S. In agreement with previous modeling studies (e.g., Meijers et al. 2007; Jayne and Marotzke 2001; Olbers and Ivchenko 2001) the ECCO2-derived MOC in the SO is dominated by an upper-ocean northward flow extending from the upwelling zone at around 65° S to the downwelling zone near 40–45° S. This flow is surface-intensified and it is associated with the Ekman transport of about 30 Sv induced by westerly winds. At depth the northward Ekman transport is compensated by a geostrophic southward flow, which is reflected by the gradual reduction of the MOC streamfunction with increasing depth. The southward flow at intermediate depths (1,500–3,500 m) carries North Atlantic Deep Water and the northward flow below 4,000 m is associated with the Antarctic Bottom Water.

Döös and Webb (1994) have shown that the deep clockwise overturning cell in the SO (Fig. 4), often referred to as the Deacon cell, does not require large unrealistic diapycnal fluxes. In particular, the downwelling near 40° S is not a cross-isopycnal flow. When the flow is integrated at constant density instead of constant depth surfaces the Deacon cell weakens or even vanishes. The existence of the deep Deacon cell is attributed to the systematic changes in the depth of density surfaces between the western boundary current region off South America and the return flow in the interior of the ocean. As a result, the zonally integrated flow in depth coordinate shows a single Deacon cell extending below 3,000 m with a stronger transport.

Although the MOC in depth coordinate illustrates the near-surface Ekman transport and its compensation at depth, it does not account for the effect of horizontal gyres and transient processes as opposed to the MOC in density coordinate (Karoly et al. 1997). The MHT by the Eulerian mean MOC is represented by the first integral term of the Eq. (2). The effect of eddies is usually described in the framework of the residual circulation theory, which first appeared in meteorology (Eliasen and Palm 1961; Andrews and McIntyre 1976) and then applied in oceanography to study the ACC dynamics (e.g., Stevens and Ivchenko 1997; Karsten et al. 2002; Marshall and Radko 2003). According to the theory, the residual circulation is the sum of the Eulerian mean flow and the flow associated with eddies. The meridional component of the residual-mean circulation thus equates to $\overline{v}_{\mathrm{res}} = \overline{v} - \frac{\partial}{\partial z}\left(\frac{\overline{v'\rho'}}{\partial\overline{\rho}/\partial z}\right)$, where the last term represents the eddy-induced circulation. The eddy-induced circulation in the SO is dominated by an anticlockwise cell

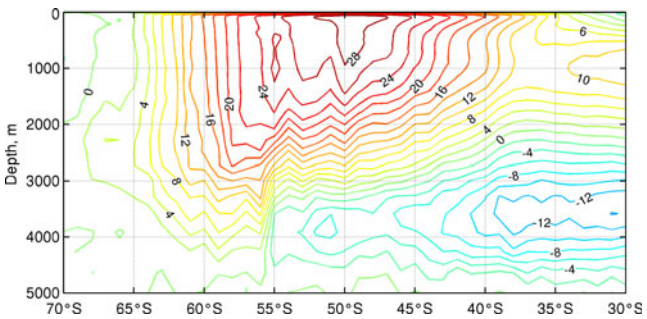


**Fig. 4** Meridional overturning circulation stream function (Sv) in depth coordinate. The separation between the streamlines is 2 Sv

that partially cancels the clockwise Deacon cell of the Eulerian mean flow (Ferreira and Marshall 2006). It is thus equivalent to the sum of the last three integral terms in the Eq. (2) and contains fluxes by the time-mean horizontal gyre (sometimes referred to as a standing eddy). Note that when the eddy-induced circulation is obtained from buoyancy fluxes across the time-mean ACC streamlines the contribution of the time-mean horizontal flow to the MHT, that is the third integral term of the Eq. (2), is missing. It has been shown, however, that when the eddy-induced flow is computed across latitude circles, the residual circulation is mainly due to the time-mean fields of the horizontal velocity and density rather than to transient eddies (Karoly et al. 1997; Stevens and Ivchenko 1997). By the virtue of Eq. (2), we do not need to use the concept of the residual circulation for the MHT computation in our study. Many recent studies have addressed the importance of the MOC in climate. The role of the MHT due to the horizontal gyre circulation, however, has not been adequately discussed in the climate-related studies of ocean circulation. It has been documented that the contribution of the horizontal gyre to the MHT is larger than that of the MOC in the subpolar oceans, where the vertical temperature gradient is generally small (Volkov et al. 2008b; Marsh et al. 2008). The horizontal gyre transport in the SO consists of the transport by the stationary oceanic gyre associated with the time-mean ACC, the transport due to the seasonal and interannual variability of the ACC, and the transport by the mesoscale eddies.

### 4.2 Heat carried by overturning, horizontal gyre, time-mean, and transients

The estimates of the components of Eq. (2) are presented in Fig. 5. The time-mean total MHT (black curve) is southward and it reaches −0.4 PW near 55° S. Similar magnitudes at this latitude were obtained from Tasmanian Partnership for Advanced Computing (TPAC) 1/8° resolution ocean model (Meijers et al. 2007) and POCM model (Jayne and Marotzke 2002). Combining hydrography using a geostrophic inverse model Ganachaud and Wunsch (2003) gave an estimate of −0.6±0.3 PW at 30° S, which is close to about −0.5 PW of the ECCO2 estimate. Much earlier Saunders and Thompson (1993) using FRAM model estimated −0.2 PW of the MHT across 60° S compared to our estimate of −0.3 PW at this latitude. Thompson's (1993) estimate of −0.15 PW at 55.25° S is twice smaller than the ECCO2 estimate.

The ECCO2 time-mean overturning circulation (red curve in Fig. 5) transports heat northward with a maximum of 0.8 PW located at about 44° S. This value is similar to the analysis of Meijers et al. (2007). Despite the large seasonal variability of the overturning circulation, the contribution of the transients in the overturning circulation to the time-mean MHT (dashed red curve in Fig. 5) is very small and can be neglected. The northward MHT by the time-mean MOC is exceeded by the southward MHT due to the horizontal circulation, leading to a net southward MHT in the SO. Most of the southward MHT is due to the time-mean horizontal circulation (blue curve in Fig. 5) reaching nearly −0.8 PW at 47° S, but the contribution of the transient processes associated with the variability of $V$ and $\theta$ (dashed blue curve in Fig. 5) is also important.

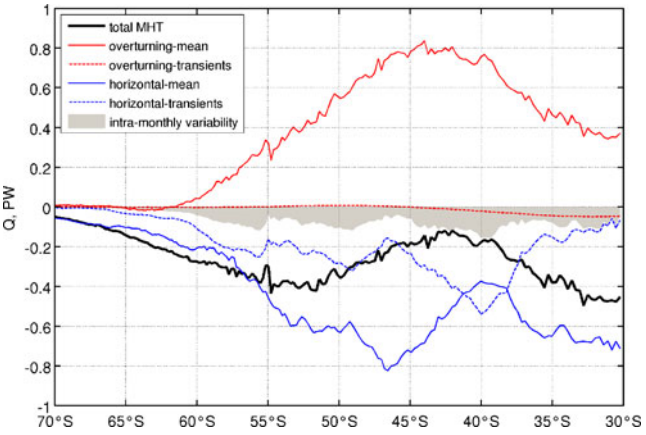


**Fig. 5** The components of the Eq. (2): the total MHT in the Southern Ocean (*solid black*), the MHT due to the transient processes associated with the intra-monthly variability of $V$ and $\theta$ (*shaded area*), the MHT due to the time-mean overturning circulation (*red*), due to transient processes related to the overturning (*dashed red*), due to the time-mean horizontal circulation (*blue*), and due to transients associated with the inter-monthly variability of the horizontal circulation plus transients associated with the intra-monthly variability of $V$ and $\theta$ (*dashed blue*)

As mentioned in Section 3, only monthly averages of $V$, $\theta$, and the product $V\times\theta$ of the model were archived. The monthly averages were computed from 6-hourly fields. The contribution of the intra-monthly variability of $V$ and $\theta$ to the MHT can be estimated by subtracting the $Q$ obtained using monthly averages of $V$ and $\theta$ from the $Q$ calculated from the monthly averaged product $V\times\theta$. This contribution is rather large (indicated by the shaded area in Fig. 5) and reaches almost −0.2 PW at 40° S. We have seen that transients associated with the inter-monthly variability of $V$ and $\theta$ contribute mainly to the MHT due to the horizontal circulation. Likewise, it is reasonable to suggest that the transients associated with the intra-monthly variability of $V$ and $\theta$ mostly contribute to the MHT due to the horizontal circulation and partly represent the eddy MHT. The dashed blue curve in Fig. 5 shows thus the sum of the MHT by transients in the horizontal circulation associated with the inter-monthly and intra-monthly variability of $V$ and $\theta$.

At 40° S the contribution of the transient processes to the horizontal gyre transport exceeds −0.5 PW (dashed blue curve in Fig. 5). This value is larger than the contribution of the time-mean horizontal gyre transport of about −0.4 PW.

The 40° S latitude goes across the Agulhas Retroflection and the Brazil-Malvinas Confluence regions, characterized by intense eddy activity. South of 41° S the relative contribution to the MHT from the time-mean horizontal circulation increases, reaching maximum at 46–47° S. Here the MHT due to the transient processes in the horizontal circulation is about −0.2 PW. Near 58° S the contributions of the transients and the mean flow are almost the same (approximately –−0.2 PW). This is the latitude of the Drake Passage—the southernmost point of the time-mean ACC streamlines (Fig. 7a)—and the relative contribution of eddies here is significant. The MHT due to transients of approximately −0.4 PW at about 40° S was also obtained by Meijers et al. (2007) and Mazloff et al. (2010). Jayne and Marotzke (2002) obtained −0.6 PW at this latitude. Further south our estimates are close to those of Mazloff et al. (2010), who also used a model constrained by observations. The estimates of Meijers et al. (2007) are approximately twice smaller, probably because of the lower vertical resolution of the TPAC model (24 depth levels). Although all these studies referred the above estimates as eddy heat transport, it should be noted, however, that in fact, these estimates (according to the way they were computed) are related to all transients, i.e., the variability on all time scales, not just mesoscale eddies. In order to estimate how much of the MHT is purely due to mesoscale eddies, a careful spatio-temporal filtering of the velocity field should be performed, which is out of the scope of the present study. A temporal filtering of the low frequency variability (retaining periods shorter than seasonal) as done in Volkov et al. (2008a) does not seem to be a good approach in the SO, because the mesoscale eddies here may have long time scales. This is evident when looking at altimeter-measured sea level averaged over long periods.

### 4.3 Geostrophic and ageostrophic components

To investigate the physical mechanisms that transport heat in the SO in more details we decomposed the meridional velocity into the geostrophic $v_{\mathrm{geos}}$ and ageostrophic $v_{\mathrm{ageos}}$ components. The full-depth geostrophic flow was computed from the model potential temperature and salinity using the surface geostrophic flow estimated from sea surface height as a reference. To conserve mass in the subsequent MHT calculation we subtracted the net flow across each zonal $x$–$z$ section and obtained the geostrophic shear flow $\tilde{v}_{\mathrm{geos}}$ (i.e., removing the barotropic component). The meridional velocity is thus locally decomposed into three constituents:

$$V(x,y,z,t) = v_{\mathrm{ageos}}(x,y,z,t) + \frac{1}{S}\iint v_{\mathrm{geos}}(x,y,z,t)\,dzdx + \tilde{v}_{\mathrm{geos}}(x,y,z,t), \quad (3)$$

where $S$ is the area of the zonal $x$–$z$ section at latitude $y$. The ageostrophic component $v_{\mathrm{ageos}}$ represents mainly the upper-ocean Ekman flow and a small ageostrophic shear associated with friction and nonlinear effects. It is compensated over the water column by the depth-averaged geostrophic flow (the second term of (3)) because the total $v$ integrates to zero across a section. Therefore, the first two terms of (3) form the Ekman component and the residual ageostrophic component, and the third term represents the geostrophic vertical and horizontal shear components.

The MHT due to the total overturning, the Ekman component, and the geostrophic vertical shear component are presented in Fig. 6a. In the SO, the total overturning MHT (black curve) is northward because the Eulerian mean MOC (Fig. 4) carries warm surface water in the Ekman layer northward, compensated by the southward return flow over the water column that has much lower temperature. This total overturning MHT is largely contributed by the Ekman component (red curve in Fig. 6a), which reaches 1 PW near 46° S. The contribution by the geostrophic vertical shear component (blue curve in Fig. 6a) is fairly small, varying from −0.2 PW at 45° S to 0.15 PW near 56° S. This is because the temperature difference between the southward flow of the North Atlantic Deep Water at intermediate depths (2,000–3,000 m) and the northward abyssal flow of the Antarctic Bottom Water is much smaller than the temperature difference between the Ekman layer and the water column below.

The poleward MHT is caused by the horizontal circulation. The poleward MHT due to the horizontal circulation exceeds −0.9 PW at around 47° S (black curve in Fig. 6b). It appears that most part of this MHT is provided by the geostrophic horizontal shear flow, i.e., the deviation of the horizontal flow from its zonal average. The MHT due to the geostrophic horizontal shear flow (blue curve in Fig. 6b) varies from −0.6 to −0.8 PW between 30–55° S. Further south the MHT due to the horizontal circulation is almost fully accomplished by the geostrophic horizontal shear flow. The contribution of the ageostrophic part of the horizontal circulation to the southward MHT (red curve in Fig. 6b) is relatively small and hardly reaches −0.2 PW near 44° S.

### 4.4 Meridional excursions of the ACC and the pathways of the MHT

We have seen that the time-mean horizontal circulation is the main contributor to the poleward MHT. This is because the ACC is not strictly zonal as illustrated in Figs. 1 and 2. Within the same depth intervals the ACC carries relatively warm water southeastward from just south of the Agulhas Retroflection to the latitudes of the Drake Passage, while the Malvinas Current carries relatively cold water equatorward. To illustrate this point, displayed in Fig. 7a is the

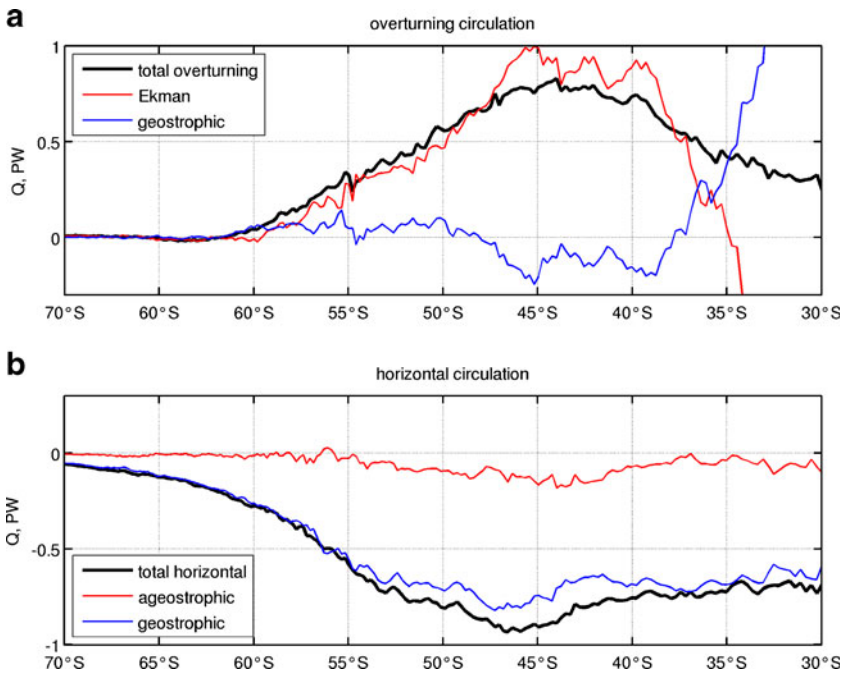


**Fig. 6** **a** The MHT due to the total overturning (*black*), due to the overturning associated with Ekman transport (*red*), and due to the geostrophic vertical shear flow (*blue*); **b** The MHT due to the total horizontal circulation (*black*), due to the ageostrophic horizontal circulation (*red*), and due to the geostrophic horizontal shear flow (*blue*)

vertical profile of the potential temperature at 45° S. Note that the temperature of the upper 1,000 m of the section where the ACC flows southeastward across 45° S is much higher than the temperature of the upper 1,000 m in the Argentine basin where the Malvinas Current flows northward. Thus, the temperature difference coupled with the meridional excursion of the ACC in these sections creates the net southward MHT.

It is instructive to illustrate the relative importance of different parts of the SO in the MHT. Unfortunately, temperature fluxes (TFs) through different parts of a latitude circle are ambiguous because the associated mass fluxes are not conserved and the absolute TF depends on the zero-temperature reference (Montgomery 1974; Hall and Bryden 1982). However, as pointed out by Lee et al. (2004), "a meaningful evaluation of the relative magnitude of temperature advection across various parts of the bounding surface of a domain is possible by considering the anomalous temperature that is advected to or from the domain. Heat advection across a partial interface can change the domain's average temperature if, and only if, the interface temperature is different from that of the domain's average." Following Lee et al. (2004), we define the TF across a latitude $y$ relative to the temperature averaged over the entire domain of the SO south of that latitude with volume $V_D$:

$$TF(x,y,t) = \int \rho C_p V(x,y,t)[\theta(x,y,t) - \langle\theta(t)\rangle]dz, \qquad (4)$$

where $\langle\theta(t)\rangle = \frac{1}{V_D}\iiint_D \theta(x, y_i < y, z, t)dxdydz$. The TF computed using (4) is independent of the reference to zero temperature because $\theta - \langle\theta\rangle$ eliminates the common reference.

The zonally cumulative depth-integrated time-mean temperature fluxes due to the geostrophic shear flow $\widetilde{v}_{\text{geos}}$ at 40° S, 45° S, and 55° S calculated using (4) illustrate which part of the SO carries most of heat (Fig. 7b). Note that the total zonal integral of (4) represents the MHT due to the geostrophic shear flow across these latitudes because $\langle\theta(t)\rangle\iiint \rho C_p \widetilde{v}_{\text{geos}}\, dxdydz = 0$. A negative/positive value of the TF indicates a warming/cooling tendency for the SO due to the southward/northward advective heat transport. Downward/upward slopes in Fig. 7b imply poleward/equatorward TF (i.e., warming/cooling tendency for the SO). At 40° S and between 20° E and 60° E the net TF is strongly southward reaching nearly −2 PW in this longitudinal band. The fluctuations in the TF are suggestive of strong mesoscale activity. This activity is associated with eddies and meanders formed in the Agulhas Retroflection area and east of it. The eastern part of the Indian sector of the SO at 40° S partly compensates for the strong southward TF in its western part. The strong southward TF associated with the ACC is also evident at 45° S between about 60° E and 100° E. The net TF in the Pacific sector of the SO at 55° S is southward and reaches approximately −1 PW. The net TF in the Atlantic sector is about 0.8 PW northward caused by the northward flowing Malvinas Current. The TF fluctuations seen at 40° S and 45° S in the Argentine Basin are associated with strong mesoscale variability in the Brazil-Malvinas Confluence region, where the northward flowing Malvinas Current collides with the southward flowing Brazil Current. This comparison exhibits the dominance of the Indian sector of the SO in transporting heat poleward. The maximum MHT due to the horizontal circulation takes place between 40° S

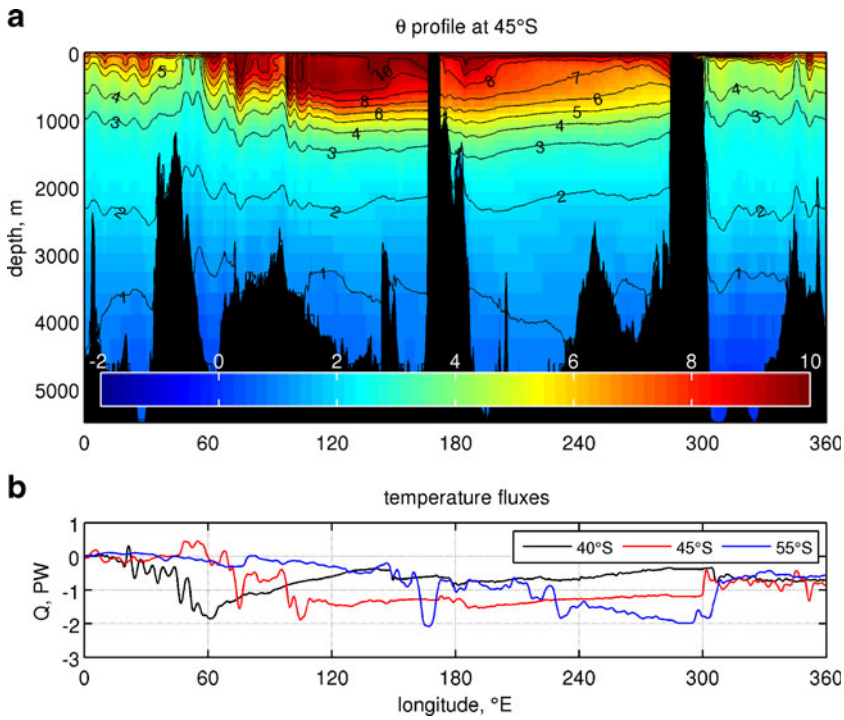


**Fig. 7** **a** Vertical profile of potential temperature (°C) at 45°S. **b** Zonally cumulative 10-year mean depth-integrated temperature flux due to the horizontal circulation along 40° S, 45° S, and 55° S

and 50° S (Fig. 6b). This latitudinal band lies in the area where the ACC in the Indian sector is directed southeastward (Fig. 1b).

## 5 Summary and discussion

In this study we used a state-of-the-art ECCO2 global ocean data synthesis at eddy-permitting resolution to study the mechanisms of the MHT in the SO. We believe that the increased resolution and accuracy of the ocean model, which is optimally constrained by observations, has allowed improved understanding of the mechanisms of the MHT.

The conclusion of the study underscores the important contribution of the horizontal circulation to the MHT in the SO. The southward MHT due to the horizontal circulation exceeds the northward MHT due to the overturning circulation, leading to a net poleward MHT. The results of the study indicate that in the SO most of the heat is transported by the time-mean overturning circulation as well as by the time-mean horizontal circulation. However, this conclusion does not contradict those from previous studies that focused on the heat transport across the time-mean streamlines or isotherms. In a hypothetical SO, in which the time-mean ACC is strictly zonal, eddy heat fluxes normal to the mean flow would have to exceed the heat flux carried by the Ekman flow and provide a net poleward heat flux to balance the heat loss at high latitudes. In this hypothetical ocean there would be no MHT by the mean flow. This is, however, not the case in the SO. The wind forcing coupled with the basin geometry and bottom topography creates the meridional variability of the ACC path. Therefore, the heat transport of the mean flow plays a significant role in the heat balance of the SO. The calculation of the MHT across latitude circles performed in the study has revealed the mechanisms of the MHT.

We have demonstrated that eddies in the SO also play a substantial role in transporting heat poleward. The transient processes associated with the horizontal circulation (eddies and seasonal/interannual variability of the ACC) have a large contribution to the total MHT. In most places the MHT due to the transient horizontal circulation amounts to approximately one third of the MHT due to the time-mean horizontal circulation. Their contribution exceeds the contribution of the time-mean horizontal circulation at 40° S—the latitude of several regions of energetic eddies. The contribution from the transient processes associated with the overturning circulation appeared to be negligible. This means that the seasonal variability of the wind stress over the SO, and hence the seasonal variability of the Ekman transport, has little effect on the time-mean MHT.

By decomposing the circulation into ageostrophic flow, its barotropic compensation, and geostrophic shear flow, we have shown that the overturning circulation associated with the wind-driven Ekman transport and the geostrophic

horizontal shear flow are the major contributors to the total MHT of the SO. The northward Ekman MHT is compensated by the southward MHT due to the geostrophic horizontal shear flow. This study explicitly highlights the importance of the geostrophic circulation of the ACC in providing the net poleward MHT in the SO.

We have demonstrated that most of the heat is carried poleward by the ACC in the Indian sector of the SO. Part of this heat is supplied by the Agulhas Current that brings warm water from the equatorial Indian Ocean. In the meantime, the warm and fresh Pacific waters are carried into the Indian Ocean through the Indonesian archipelago. By conducting numerical experiments with open and closed Indonesian passages, Lee et al. (2002) showed that the blockage of the Indonesian throughflow cuts off the heat transport from the Pacific to the Indian Ocean, weakens the South Equatorial Current and the Agulhas Current, and strengthens the East Australian Current. It is therefore conceivable that the MHT in the SO is affected by the Indonesian throughflow on relatively long time scales, a subject that requires further investigation.

**Acknowledgments** This research was carried out at the Jet Propulsion Laboratory, California Institute of Technology, within the framework of the ECCO2 project, sponsored by the National Aeronautics and Space Administration. The efforts of all the members of the ECCO2 group, in particular, Dimitris Menemenlis and Hong Zhang, who have performed model simulations are greatly appreciated.



## References

Andrews DG, McIntyre ME (1976) Planetary waves in horizontal and vertical shear: the generalized Eliassen-Palm relation and the mean zonal acceleration. J Atmos Sci 33:2031–2048

Bryan K (1982) Poleward heat transport by the ocean: observations and models. Annu Rev Earth Planet Sci 10:15–38

Bryden HL (1979) Poleward heat flux and conversion of available potential energy in Drake Passage. J Mar Res 37(1):1–22

Bryden HL, Heath RA (1985) Energetic eddies at the northern edge of the Antarctic Circumpolar Current. Prog Oceanogr 14:65–87

Chelton DB, deSzoeke RA, Schlax MG, Naggar KE, Siwertz N (1998) Geographical variability of the first baroclinic Rossby Radius of Deformation. J Phys Oceanogr 28:433–460

Cunningham SA, Alderson SG, King BA, Brandon MA (2003) Transport and variability of the Antarctic Circumpolar Current in Drake Passage. J Geophys Res 108(C5):8084. doi:10.1029/2001JC001147

de Szoeke RA, Levine MD (1981) The advective flux of heat by mean geostrophic motions in the Southern Oceans. Deep-Sea Res 28:1057–1085

Döös K, Webb DJ (1994) The Deacon cell and the other meridional cells in the Southern Ocean. J Phys Oceanogr 24:429–442

Eliasen A, Palm E (1961) On the transfer of energy in stationary mountain waves. Geophys Publ 22:1–23

Ferreira D, Marshall J (2006) Formulation and implementation of a "residual-mean" ocean circulation model. Ocean Model 13:86–107

Fu L-L (2009) Pattern and velocity propagation of the global ocean eddy variability. J Geosphys Res 114:C11017. doi:10.1029/2009JC005349

Ganachaud A, Wunsch C (2000) Improved estimates of global ocean circulation, heat transport and mixing from hydrographic data. Nature 408:453–457

Ganachaud A, Wunsch C (2003) Large-scale ocean heat and freshwater transports during the World Ocean Circulation Experiment. J Climate 16:696–705

Hall MM, Bryden HL (1982) Direct estimates and mechanisms of ocean heat transport. Deep-Sea Res 29:339–359

Ivchenko VO, Richards KJ, Stevens DP (1996) The dynamics of the Antarctic Circumpolar Current. J Phys Oceanogr 26:753–774

Jayne S, Marotzke J (2001) The dynamics of ocean heat transport variability. Rev Geophys 39:385–411

Jayne S, Marotzke J (2002) The oceanic eddy heat transport. J Phys Oceanogr 32:3328–3345

Johnson GC, Bryden HL (1989) On the size of the Antarctic Circumpolar Current. Deep-See Res 36:39–53

Karoly DJ, McIntosh PC, Berrisford P, McDougall TJ, Hirst AC (1997) Similarities of the Deacon cell in the Southern Ocean and Ferrel cells in the atmosphere. Q J R Meteorol Soc 123:519–526

Karsten R, Jones H, Marshall J (2002) The role of eddy transfer in setting the stratification and transport of a circumpolar current. J Phys Oceanogr 32:39–54

Large WG, McWilliams JC, Doney S (1994) Oceanic vertical mixing: A review and a model with a nonlocal boundary layer parameterization. Rev Geophys 32:363–403

Lee MM, Coward A (2003) Eddy mass transport for the Southern Ocean in an eddy-permitting global ocean model. Ocean Model 5:249–266

Lee T, Fukumori I, Menemenlis D, Xing Z, Fu LL (2002) Effects of the Indonesian throughflow on the Pacific and Indian Oceans. J Phys Oceanogr 32:1404–1429

Lee T, Fukumori I, Tang B (2004) Temperature advection: internal versus external processes. J Phys Oceanogr 34:1936–1944

Marsh R, Josey SA, de Cuevas BA, Redbourn LJ, Quartly GD (2008) Mechanisms for recent warming of the North Atlantic: insights gained with an eddy-permitting model. J Geophys Res 113: C04031. doi:10.1029/2007JC004096

Marshall J, Radko T (2003) Residual-mean solutions for the Antarctic Circumpolar Current and its associated overturning circulation. J Phys Oceanogr 33:2341–2354

Marshall J, Adcroft A, Hill C, Perelman L, Heisey C (1997) A finite volume, incompressible Navier-Stokes model for studies of the ocean on parallel computers. J Geophys Res 102:5753–5766

Mazloff MR, Heimbach P, Wunsch C (2010) An Eddy-permitting Southern Ocean State estimate. J Phys Oceanogr

Meijers A, Bindoff NL, Roberts JL (2007) On the total, mean, and eddy heat and freshwater transports in the Southern Hemisphere of a 1/8 × 1/8 global ocean model. J Phys Oceanogr 37:277–295

Menemenlis D, Fukumori I, Lee T (2005) Using Green's functions to calibrate an ocean general circulation model. Mon Weather Rev 133:1224–1240

Montgomery RB (1974) Comment on "Seasonal variability of the Florida Current" by Niiler and Richardson. J Mar Res 32:533–535

Munk WH, Palmén E (1951) Note on the dynamics of the Antarctic Circumpolar Current. Tellus 3:53–55

Olbers D, Ivchenko VO (2001) On the meridional circulation and balance of momentum in the Southern Ocean of POP. Ocean Dyn 52:79–93

Phillips HE, Rintoul SR (2000) Eddy variability and energetics from direct current measurements in the Antarctic Circumpolar Current south of Australia. J Phys Oceanogr 30:3050–3076

Rintoul SR, Hughes C, Olbers D (2001) The Antarctic Circumpolar Current System, Chapter 4.6. In: Siedler G et al. (eds) Ocean Circulation and Climate, International Geophysics Series, vol 77. pp 271–302

Saunders PM, Thompson SR (1993) Transport, heat, and fresh water fluxes within a diagnostic numerical model (FRAM). J Phys Oceanogr 23:452–464

SSALTO/DUACS User Handbook (2009) M(SLA) and M(ADT) near-real time and delayed time products, Aviso Altimetry (www.aviso.oceanobs.com)

Stevens DP, Ivchenko VO (1997) The zonal momentum balance in an eddy-resolving general circulation model of the Southern Ocean. Q J R Meteorol Soc 123:929–951

Sun C, Watts DR (2002) Heat flux carried by the Antarctic Circumpolar Current mean flow. J Geophys Res 107(C9):3119. doi:10.1029/2001JC001187

Thompson SR (1993) Estimation of the transport of heat in the Southern Ocean using a fine-resolution numerical model. J Phys Oceanogr 23:2493–2497

Volkov DL, Lee T, Fu L-L (2008a) Eddy-induced meridional heat transport in the ocean. Geophys Res Lett 35:L20601. doi:10.1029/2008GL035490

Volkov DL, Fu L-L, Lee T (2008b) Meridional heat transports in the ocean from an ECCO2 data synthesis. Eos Trans AGU 89(53), Fall Meet. Suppl., Abstract OS31C-1294

Webb DJ, et al (1991) The FRAM atlas of the Southern Ocean, Natural Environment Research Council, 67 pp

Whitworth T III, Peterson RG (1985) Volume transport of the Antarctic Circumpolar Current through Drake Passage. J Phys Oceanogr 15 (6):810–816